A Single Crystal EPR and ESEEM Analysis of Cu(II)-Doped Bis(L-histidinato)cadmium Dihydrate

Michael J. Colaneri* and Jack Peisach

Contribution from the Department of Molecular Pharmacology, Albert Einstein College of Medicine, 1300 Morris Park Avenue, Bronx, New York 10461

Received January 20, 1995[⊗]

Abstract: A study was undertaken to investigate the nature of the hyperfine and quadrupole coupling parameters of the distant ^{14}N in Cu(II)-coordinated imidazole in bis(L-histidinato)cadmium dihydrate (I) to further our understanding of the ESEEM patterns obtained for copper proteins, where Cu(II) is coordinated to either Nδ or Nϵ. Single crystal EPR data have been collected at 77 K in isotopically enriched ^{63}Cu-doped crystals grown from D_2O in order to obtain g and Cu(II) hyperfine tensors. From the obtained spectra, hyperfine splittings from two directly coordinated ^{14}N nuclei are evident. Single crystal ESEEM measurements at 4.2 K were used to determine the hyperfine and quadrupole tensors of the remote $^{14}N\epsilon$ of the imidazole group ligated to the Cu(II). These tensors can be compared to those previously obtained for $^{14}N\delta$ in Cu(II)-doped L-histidine HCl H_2O (II) (Colaneri, M. J.; Peisach, J. *J. Am. Chem. Soc.* **1992**, 114, 5335.). The remote ^{14}N hyperfine tensor found in I is very similar to that previously obtained in II, displaying predominantly a rhombic anisotropy, 0.36, −0.10, −0.26 MHz, and suggesting that this form should exist for similar histidine ligated copper sites in proteins. The hyperfine isotropy in I, 1.61 MHz, is, however, slightly larger than that found in II, 1.35 MHz. The derived quadrupole coupling parameters e^2qQ/h and η have values of −1.57 MHz and 0.64, respectively, with the maximum principal component occurring normal to the imidazole plane. This tensor is different from that previously found in II and may reflect the different hydrogen bonding environments of the remote nitrogen in the host crystal systems. The present ESEEM study shows that a single imidazole coordinates to the Cu(II). From these results, a Cu(II) binding site is postulated whereby the metal ion ligates to two equatorial nitrogens and an axial carboxylate oxygen from a single histidine molecule. A carboxylate oxygen from a neighboring histidine is most likely positioned trans to the imidazole nitrogen ligand perhaps by a small movement about its $C_\alpha-C_\beta$ bond. This type of complex is thought to be less stable than the more usually observed, four-equatorial ligand complex. The temperature dependence of the EPR spectra of I is consistent with this notion. The EPR parameters observed at room temperature are found to represent the dynamic average of the g and ^{63}Cu hyperfine tensors measured at 77 K. These sets of low temperature tensors correspond to copper sites bound to neighboring histidine molecules. The averaging is believed to occur by the copper hopping between these sites at higher temperatures.

Introduction

Electron spin echo envelope modulation (ESEEM) spectroscopy provides structural information about weakly coupled nuclei in the vicinity of a paramagnetic species. To aid in the analysis and understanding of ESEEM patterns obtained from copper proteins, single crystal ESEEM was employed to accurately determine the ^{14}N hyperfine and quadrupole tensors of the remote nitrogen of Cu(II) coordinated imidazole in doped bis(L-histidinato)cadmium dihydrate. The metal coordination to the imidazole of histidine in the bis(L-histidinato)cadmium dihydrate complex serves as a model for type-I copper sites in that the ligation is through the Nδ nitrogen. Cu(II)-doped L-histidine HCl H_2O, on the other hand, served as a model for type-II copper sites because of the usual metal coordination to the imidazole Nϵ.[1−3] Interest in comparing the quadrupole parameters for these two systems stems from a recent suggestion that differences in quadrupole parameters for the remote nitrogen of histidine imidazole in copper proteins may be due to the inequivalence of the nitrogens.[4]

In two previous ESEEM studies on similar Cu(II)−imidazole complexes, Cu(II)-doped Zn(II) bis(1,2−dimethylimidazole)-dichloride[5] and Cu(II)-doped L-histidine HCl H_2O,[3] the ^{14}N quadrupole tensor was shown to be correlated with imidazole geometry. On the other hand, the structural correlation of the hyperfine tensor is not so clearly defined since in only one of these studies, that of Cu(II)-doped L-histidine HCl H_2O, is there a correspondence with the ligand bonding geometry. That the hyperfine tensor did not have any predictable directions in Cu(II)-doped Zn(II) bis(1,2−dimethylimidazole)dichloride may have been a consequence of the poorly understood copper unpaired electron distribution in the tetrahedral complex. In contrast, the predominantly d_{z^2} unpaired copper orbital in Cu(II)-doped L-histidine HCl H_2O presented a simpler image of the unpaired electron distribution to the axially bound imidazole. The ^{14}N hyperfine interaction in the doped L-histidine HCl H_2O system was of particular interest because of the predominantly rhombic form (A, 0, −A) that it displayed. A delocalized model of unpaired spin offered a reasonable explanation of the tensor components in this system.[3] This potential generality prompted the undertaking of the present study in order to examine the hyperfine anisotropy of the imidazole remote nitrogen in a copper−histidine complex which exhibits a different metal coordination linkage for imidazole.

[⊗] Abstract published in *Advance ACS Abstracts*, June 1, 1995.

(1) Hirasawa, R.; Kon, H. *J. Chem. Phys.* **1972**, *56*, 4467.

(2) McDowell, C. A.; Naito, A.; Sastry, D. L.; Cui, Y. U.; Sha, K.; Yu, S. X. *J. Mol. Struct.* **1989**, *185*, 361.

(3) Colaneri, M. J.; Peisach, J. *J. Am. Chem. Soc.* **1992**, *114*, 5335.

(4) Goldfarb, D.; Fauth, J.-M.; Farver, O.; Pecht, I. *Appl. Magn. Reson.* **1992**, *3*, 333.

(5) Colaneri, M. J., Potenza, J. A., Schugar, H. J. and Peisach, J. *J. Am. Chem. Soc.* **1990**, *112*, 9451.

0002-7863/95/1517-6308$09.00/0

X-ray diffraction analysis has been carried out on numerous copper-histidine amino acid complexes,[6-14] although only two have been performed on copper bis-histidine crystals.[9,12] The histidine molecule in these crystal structures usually acts as a bidentate ligand with the metal being bound to imidazole and amino nitrogens. Owing to its biological interest, numerous magnetic resonance studies have been undertaken in order to define the mode of metal coordination in solutions at room temperature and when frozen.[15-25] Electron paramagnetic resonance (EPR) spectroscopy has also been used to quantitate the relative amounts of different Cu(II)–histidine complexes that can coexist in solution.[20,22,24,25] A most interesting result from these studies is the observation of a switch of copper ligands upon freezing.[22] Specifically, copper in excess histidine ligates to both one and two imidazole nitrogens in solution,[22] but the predominant form at low temperature is a four imidazole–nitrogen coordinated complex.[20] As pointed out, competition between ligand types may result in misleading structural information from spectroscopic analysis of frozen solution samples.[22] Single crystal EPR has been used to investigate only one copper-histidine complex, namely, Cu(II)-doped L-histidine HCl H_2O.[1,2] Here, the copper-ligand geometry is found to be approximately trigonal bipyrimidal, resulting in a predominantly d_{z^2} ground state.[1,2] The present system has parameters consistent with a more commonly observed $d_{x^2-y^2}$ ground state, and its analysis thus adds to the basic understanding of copper–histidine complexes.

Experimental Section

Crystals of bis-(L-histidinato)cadmium dihydrate doped with Cu(II) were grown by the slow evaporation of an aqueous solution of L-histidine (Aldrich) and cadmium carbonate (Alfa Chemicals) in a 2:1 molar ratio, containing 1–2 mol % copper carbonate (Aldrich). Crystals having their labile hydrogens exchanged with deuteriums were grown from D_2O (MSD). A few experiments were performed on doped crystals with the imidazole Cϵ proton replaced with deuterium. This exchange was accomplished according to published procedures[26] by heating L-histidine in D_2O at ≈65 °C for one week with the solution adjusted to pH ≈ 8 with NaOH. ^{63}Cu (99.9% enrichment) was obtained from Isotec, Inc. The crystals exhibited habits consistent with published work.[27] Magnetic resonance spectra were measured as a function of magnetic field orientation in planes bound by the crystallographic axes. For EPR measurements, crystal samples were attached (Duco cement) to the end of glass pipets, aligned using crystal morphology observed with a magnifying lens, and inserted into conventional 3 × 4 mm EPR tubes. EPR experiments were performed at X-band (9 GHz) at 77 K. Some experiments were done at Q-band (34 GHz) at 100 K using a Bruker 300 ESR spectrometer.

Single crystal EPR measurements were performed on a Varian E-112 spectrometer whose magnet was equipped with a rotatable base. The rectangular TE102 cavity that was utilized restricted the magnet from rotating more than ±20°, and manual sample reorientation was therefore necessary during data collection. Severe spectral overlap limited the orientations at which data could be measured, and this was only partially circumvented by pulsed-EPR methods.[28] Measured data were used to fit the g and copper hyperfine tensor parameters according to a least-squares criteria. Calculations were accomplished utilizing modified software which had been written previously for the single crystal ESR/ENDOR analysis of free radicals.[29] Only the first three terms in the spin hamiltonian (eq 1) were used to describe the angular dependence of the EPR spectra. Terms in eq 1 have been previously specified.[30] Symmetric tensors in eq 1 were assumed throughout. The adjustable parameters in this analysis were six g-tensor (g) elements and six copper hyperfine-tensor (A^{Cu}) elements. The procedure is derived from an algorithm employed in the fitting of nuclear magnetic resonance data[31] with the additional assumption that the vector of residuals is proportional to the differences between the measured and calculated resonant magnetic fields.

$$\mathcal{H} = \beta S \cdot g \cdot H + I^{Cu} \cdot A^{Cu} \cdot S - g_n{}^{Cu}\beta_n H \cdot I^{Cu} + I^N \cdot A^N \cdot S - g_n{}^N \beta_n H \cdot I^N + I^N \cdot Q^N \cdot I \quad (1)$$

ESEEM experiments were carried out on a home-built X-band pulsed-EPR spectrometer previously described[32] and three-pulse ESE decay patterns were measured and treated as reported earlier.[3,5] Crystals grown in H_2O were cemented directly onto the side wall of a microwave cavity described by Mims.[33] All ESEEM experiments were done at 4.2 K. The ^{14}N modulation frequencies in the fourier transformed ESEEM pattern (FT-ESEEM) were followed as a function of magnetic field orientation in the crystal planes. These data were used to least-squares fit the six hyperfine (A^N) and five quadrupole tensor (Q^N) parameters of the coupled ^{14}N using eq 1 following procedures previously outlined.[3,5] The intensities of the modulation frequencies in the FT-ESEEM spectra were simulated using Mims' equations.[34,35] Eigenvectors derived from the complete Hamiltonian (eq 1) were utilized in these computations. This procedure provided a better comparison to the observed FT-ESEEM intensities since there were small dependencies of the calculated ^{14}N FT-ESEEM lines on the copper nuclear spin state.

Results

Crystal Structure and EPR Spectra. The crystal structure of bis-(L-histidinato)cadmium dihydrate has been determined

(6) Blount, J. F.; Fraser, K. A.; Freeman, H. C.; Szymanski, J. T.; Wang, C.-H. *Acta Crystallogr.* **1967**, *22*, 396.
(7) Freeman, H. C.; Szymanski, J. T. *Acta Crystallogr.* **1967**, *22*, 406.
(8) Freeman, H. C.; Guss, J. M.; Healy, M. J.; Martin, R.-P.; Nockolds, C. E. *Chem. Comm.* **1969**, 225.
(9) Evertsson, B. *Acta Crystallogr.* **1969**, B25, 30.
(10) Osterberg, R.; Sjoberg, B.; Soderquist, R. *Acta Chem. Scand.* **1972**, *26*, 4184.
(11) Camerman, N.; Camerman, A.; Sakar, B. *Can. J. Chem.* **1976**, *54*, 1309.
(12) Camerman, N.; Fawcett, J. K.; Kruck, T. P. A.; Sakar, B.; Camerman, A. *J. Am. Chem. Soc.* **1978**, *100*, 2690.
(13) Ono, T.; Shimanouchi, H.; Sasada, Y.; Sakurai, T.; Yamauchi, O.; Nakahara, A. *Bull. Chem. Soc. Jpn.* **1979**, *52*, 2229.
(14) Ono, T.; Sasada, Y. *Bull. Chem. Soc. Jpn.* **1981**, *54*, 90.
(15) Crawford, T. H.; Dalton, J. O. *Arch. Biochemistry Biophys.* **1969**, *131*, 123.
(16) Rotillo, G.; Calabrese, L. *Arch. Biochemistry Biophys.* **1971**, *143*, 218.
(17) Voelter, W.; Sokolowski, G.; Weber, U.; Weser, U. *Eur. J. Biochemistry* **1975**, *58*, 159.
(18) Brown, C. E.; Antholine, W. E.; Froncisz, W. *J. Chem. Soc., Dalton Trans.* **1980**, 590.
(19) Valensin, G.; Basosi, R.; Antholine, W. E.; Gaggelli, E. J. *Inorg. Biochemistry* **1985**, *23*, 125.
(20) Basoi, R.; Valensin, G.; Gagelli, E.; Froncisz, W.; Pasenkiewicz-Gierula, M.; Antholine, W. E.; Hyde, J. S. *Inorg. Chem.* **1986**, *25*, 3006.
(21) McPhail, D. B.; Goodman, B. A. *J. Chem. Soc., Faraday Trans. 1* **1987**, *83*, 3683.
(22) Pasenkiewicz-Gierula, M.; Froncisz, W.; Basoi, R.; Antholine, W. E.; Hyde, J. S. *Inorg. Chem.* **1987**, *26*, 801.
(23) Romanelli, M.; Basosi, R. *Chem. Phys. Lett.* **1988**, *143*, 404.
(24) Szabo-Planka, T.; Rockenbauer, A.; Gyor, M.; Gaizer, F. *J. Coord. Chem.* **1988**, *17*, 69.
(25) Pogni, R.; Lunga, G. D.; Basosi, R. *J. Am. Chem. Soc.* **1993**, *115*, 1546.
(26) Matsuo, H.; Ohe, M.; Sakiyama, F.; Narita, K. *J. Biochemistry* **1972**, *72*, 1057. Krieger, M.; Koppe II, R. E.; Stroud, R. M. *Biochemistry* **1976**, *15*, 3458.
(27) Fuess, H.; Bartunik, H. *Acta Crystallogr.* **1976**, *B32*, 2803.
(28) Colaneri, M. J. and Peisach, J. *J. Mag. Res.* **1993**, *A102*, 360.
(29) Colaneri, M. J.; Box, H. C. *J. Chem Phys.* **1986**, *84*, 1926.
(30) Wertz, J. E.; Bolton, J. R. In *Electron Spin Resonance: Elementary Theory and Practical Applications*; McGraw-Hill, Inc.: New York, 1972.
(31) Castellano, S.; Bothner-By, A. A. *J. Chem. Phys.* **1964**, *41*, 3863.
(32) McCracken, J.; Peisach, J.; Dooley, D. M. *J. Am. Chem. Soc.* **1987**, *109*, 4064.
(33) Mims, W. B. *Phys. Rev.* **1964**, *133*, A835.
(34) (a) Mims, W. B. *Phys. Rev.* **1972**, *B6*, 3543. (b) Mims, W. B. *Phys. Rev.* **1972**, B6, 2409.
(35) Reijerse, E. J.; Paulissen, M. L. H.; Keijzers, C. P. *J. Magn. Reson.* **1984**, 60, 66.

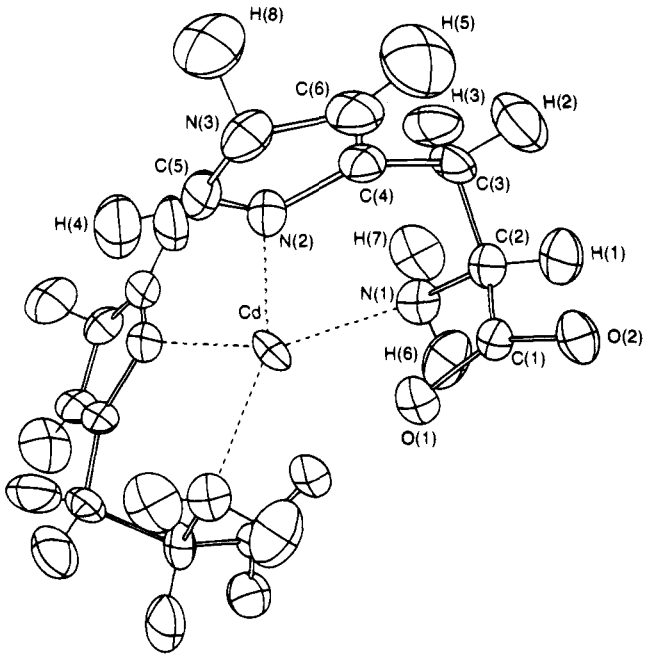

Figure 1. View of the crystal structure of bis(L-histidinato)cadmium dihydrate[27] (reproduced in a modified form with permission of the authors). The cadmium sits on the two-fold axis along the *ab* plane diagonal. The metal-coordinated histidine molecules are related by this rotation axis.

first by X-ray[36] and later by neutron diffraction[27] methods. Figure 1 shows the spatial arrangement of the complex in the crystal structure. Crystals have space group $P4_32_12$, with $a = b = 7.397$ Å and $c = 30.53$ Å.[27] In this space group, the *a* and *b* axes are indistinguishable, and axis labels in the figures that follow are arbitrary. The unit cell consists of four cadmium and eight histidine molecules. Two histidine molecules bind the cadmium ion with the coordination geometry being described as a slightly flattened tetrahedron. These two molecules are related by a two-fold rotation axis positioned along the diagonal of *a* and *b*. The cadmium ion sits on this two-fold axis and thus occupies a special position in the unit cell. Each histidine is ligated to the metal through an amide nitrogen (Cd−N(1) bond length = 2.287 Å), an imidazole nitrogen (Cd-N(2) bond length = 2.290 Å) and one carboxylate oxygen (Cd-O(1) bond length = 2.480 Å) at a further distance.

EPR spectra at 77 K of ^{63}Cu-doped crystals grown from D_2O, taken while the applied field is aligned along the crystallographic axis are shown in Figure 2. One four-line, copper ($I = 3/2$) hyperfine split pattern is seen when the field is applied along the crystallographic *c* axis (*c*//H). The spectra measured at *a*//H or *b*//H (*a,b*//H) show two partly resolved, four-line copper hyperfine split patterns. The low field species is labeled A and the high field species is labeled B. The spectra observed with H either along *a* or *b* are identical. Were the copper in a special position, the EPR spectra would show only one species with H along the *a* and *b* axes. Thus, the copper does not isomorphously substitute for the cadmium in the crystal. This is not totally unexpected given the large differences in the crystal ionic radii[37] for Cd(II) (0.97 Å) and Cu(II) (0.72 Å).

The ^{63}Cu hyperfine split resonance fields were measured as a function of applied field orientation in the reference planes and are depicted in Figure 3. The EPR orientational dependencies show that these two species interchange in the *ab* plane,

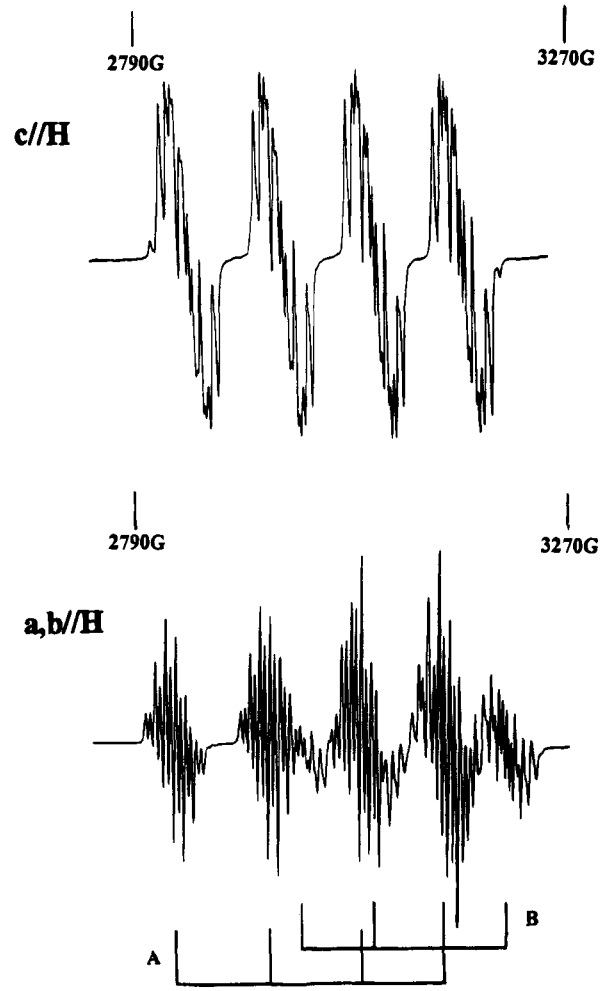

Figure 2. X-band EPR spectra observed from deuterated single crystals of ^{63}Cu(II)-doped bis(L-histidinato)cadmium at 77 K. The upper trace was taken with the static magnetic field (H) positioned along the crystallographic *c* axis, *c*//H, the lower trace when the magnetic field was along either the *a* or *b* axes, *a,b*//H. One site is present when *c*//H, two sites; labeled A and B corresponding to the low and high field patterns, respectively, are evident when *a,b*//H.

with a two-fold symmetry axis being present along the plane diagonal. These observations are consistent with the 422 point group symmetry of the host crystal. Table 1 summarizes the results of the EPR measurements and tensor refinements. The solid curves in Figure 3 represent the orientation dependence of resonant fields calculated using the tensors in Table 1. The maximum component of the copper hyperfine tensor was assumed to be negative. The tensor off-diagonal sign choice was confirmed by comparing the derived tensors with the Q-band EPR spectra of crushed crystals. The least-square calculation exhibited a slightly ill-behaved refinement. In particular, the A_x hyperfine principal component oscillated about 0 Mhz. With the exception of this parameter, the others remained essentially unchanged during this part of the calculation, i.e., the principal axes and values changed by less than 5° and 2 MHz, respectively. It was decided to terminate the refinement at the minimum root-mean-square (rms) deviation observed for the data (3.7 G). The *g* and *A* tensors listed in Table 1 are one set of eight pairs of tensors that are related by the point group symmetry and therefore refer to one of the eight symmetric sites in the crystal structure. Direction cosines α, β, and γ within these eight sites have the following symmetry relationships: $\alpha\beta\gamma$, $-\alpha-\beta\gamma$, $-\alpha\beta-\gamma$, $\alpha-\beta-\gamma$, $\beta\alpha\gamma$, $-\beta-\alpha\gamma$, $-\beta\alpha-\gamma$, and $\beta-\alpha-\gamma$.

(36) Candlin, R.; Harding, M. M. *J. Chem. Soc.* **1967**, 421.
(37) *Handbook of Chemistry and Physics*; Weast, R. C., Ed.; CRC Press Inc.: Cleveland, OH, 1974; p F-198.

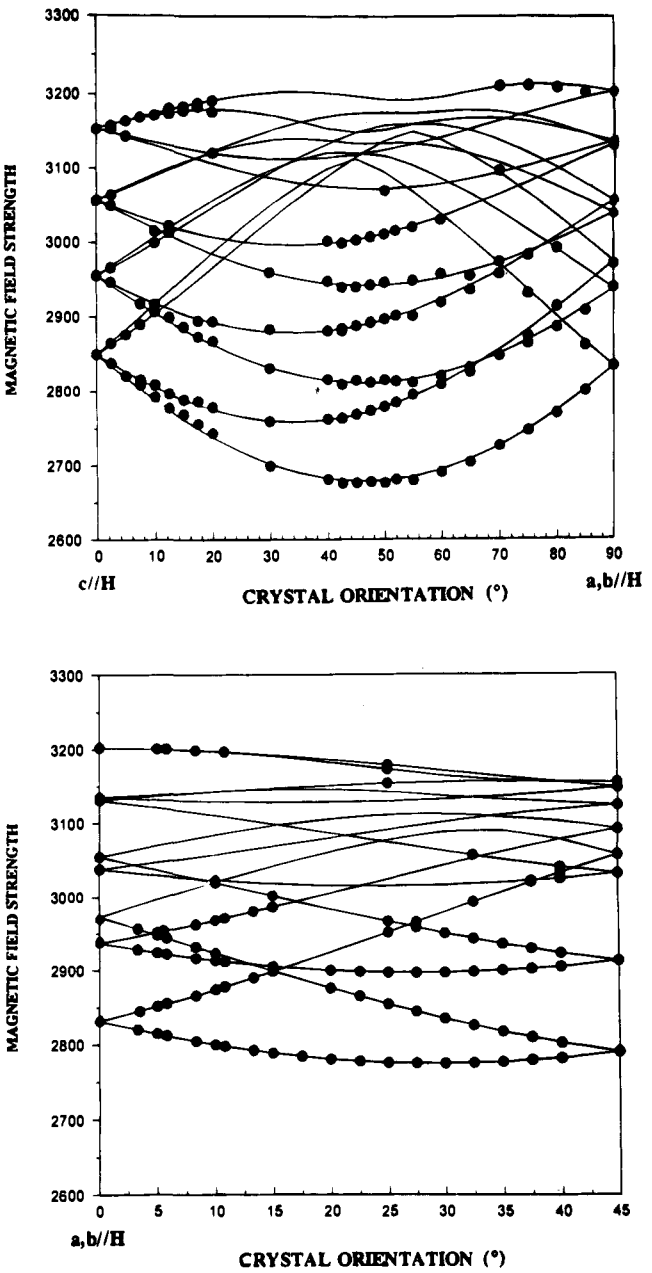

Figure 3. Plots illustrating the dependencies of the resonant magnetic fields of the copper hyperfine splittings on the crystal orientation with respect to H in the planes referenced by the crystallographic axes. The top plot is the dependence in the plane bound by the *c* axis and either the *a* or *b* axes; the bottom plot is with H oriented in the ab plane. Solid curves are calculated dependencies using the tensor parameters in Table 1.

Consistent with previously analyzed copper-doped amino acid single crystal systems,[38-43] the *g* and copper hyperfine tensors in Table 1 indicate a predominantly $d_{x^2-y^2}$ unpaired orbital ground state. The orientations of the *g* and copper hyperfine tensors have good correlation with the direction of the largest *g*-value (g_z) corresponding to the largest hyperfine (A_z) direction to within 3°. The other two tensor directions also show good correspondence but are not exactly aligned with one another, the deviations between the g_x and A_x axes, and the g_y and A_y axes each being ≈25°. These tensor principal values and the approximate correspondence of the principal directions suggest a dominant square planar crystal field. The copper ligands are expected to be positioned roughly in the *xy* plane, taking up equatorial positions, i.e., along the *x* and *y* directions. The low symmetry of the copper site may result in the noncolinearity of the *x* and *y* component directions of the two tensors.[44]

Table 1. *g* and ^{63}Cu Hyperfine Tensors Obtained at 77 K from EPR Measurements on Single Crystals of Cu(II)-Doped Bis(l-histidinato)cadmium Dideuterate

	direction cosines		
principal values	*a*	*b*	*c*
	g-Tensor		
2.299	0.6427	0.4032	−0.6514
2.092	−0.7414	0.5414	−0.3965
2.048	0.1928	0.7378	0.6469
	^{63}Cu Hyperfine Tensor (MHz)		
−456.1	0.634	0.444	−0.633
65.6	−0.627	0.774	−0.086
−0.6	0.452	0.452	0.769

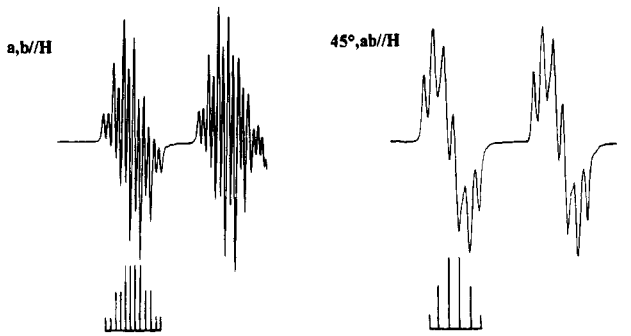

Figure 4. An expanded diagram of the EPR spectra of the low field portions of species A at *a,b*//H (left) and with H in the ab plane at an angle of 45° from the *a* (or *b*) axis (right). The 12 line pattern of species A in the left spectrum can be modeled by two nonequivalent 1:1 doublets with splittings of 5 and 12 G and two equivalent 1:1:1 triplets with splittings of 12 G. The six-line pattern in the right spectrum can be explained by two equivalent 1:1:1 triplets and a 1:1 doublet each having splittings of 12 G. The triplets arise from interactions of two ^{14}N nuclei.

The additional EPR hyperfine structure of each copper split line are further depicted in Figures 3 and 4. The structure is complicated over most of the angular settings and consist of 12, 14, and 13 lines at *a,b*//H (species A), *a,b*//H (species B), and at *c*//H, respectively. The descriptions of these patterns were consistently modeled with two sets of nonequivalent 1:1:1 triplet and 1:1 doublet splittings. Stick patterns generated using measured splittings are displayed beneath experimental EPR spectra in Figure 4 at *a,b*//H (species A) and with H at 45° from *a,b*//H in the *ab* plane. The two triplet splittings arise from two ^{14}N nuclei ($I = 1$) that couple the unpaired spin. These splittings vary from 8.5−13 Gauss (G) in the rotational spectra and are thus in the range determined by electron-nuclear double resonance (ENDOR) for amino acid nitrogens directly coordinated to Cu(II).[2,41,45-47]

The smaller of the two doublets exhibits a splitting of 15 MHz at *a,b*//H (species A). A potential coupling assignment is to a proton ($I = 1/2$) attached to the C_α carbon atom (C2). Hyperfine couplings from protons bound to the C_α carbon have

(38) Windsch, W.; Weltner, M. *Z. Naturforsch.* **1967**, *22a*, 1.
(39) Fujimoto, M.; Janecka, J. *J. Chem. Phys.* **1971**, *55*, 1152.
(40) Fujimoto, M.; Saito, S.; Tomkiewicz, Y. *Bioinorg. Chem.* **1973**, *2*, 341.
(41) Wartewig, S.; Bottcher, R.; Windsch, W. *Chem. Phys.* **1981**, *58*, 211.
(42) McDowell, C. A.; Naito, A.; Sastry, D. L.; Cui, Y.; Sha, K. *J. Phys. Chem.* **1990**, *94*, 8113.
(43) Steren, C. A.; Calvo, R.; Piro, O. E.; Rivero, B. E. *Inorg. Chem.* **1989**, *28*, 1933.
(44) Pilbrow, J. R. *Transition Ion Electron Paramagnetic Resonance*; Clarendon Press: Oxford, 1990; pp 161−165.

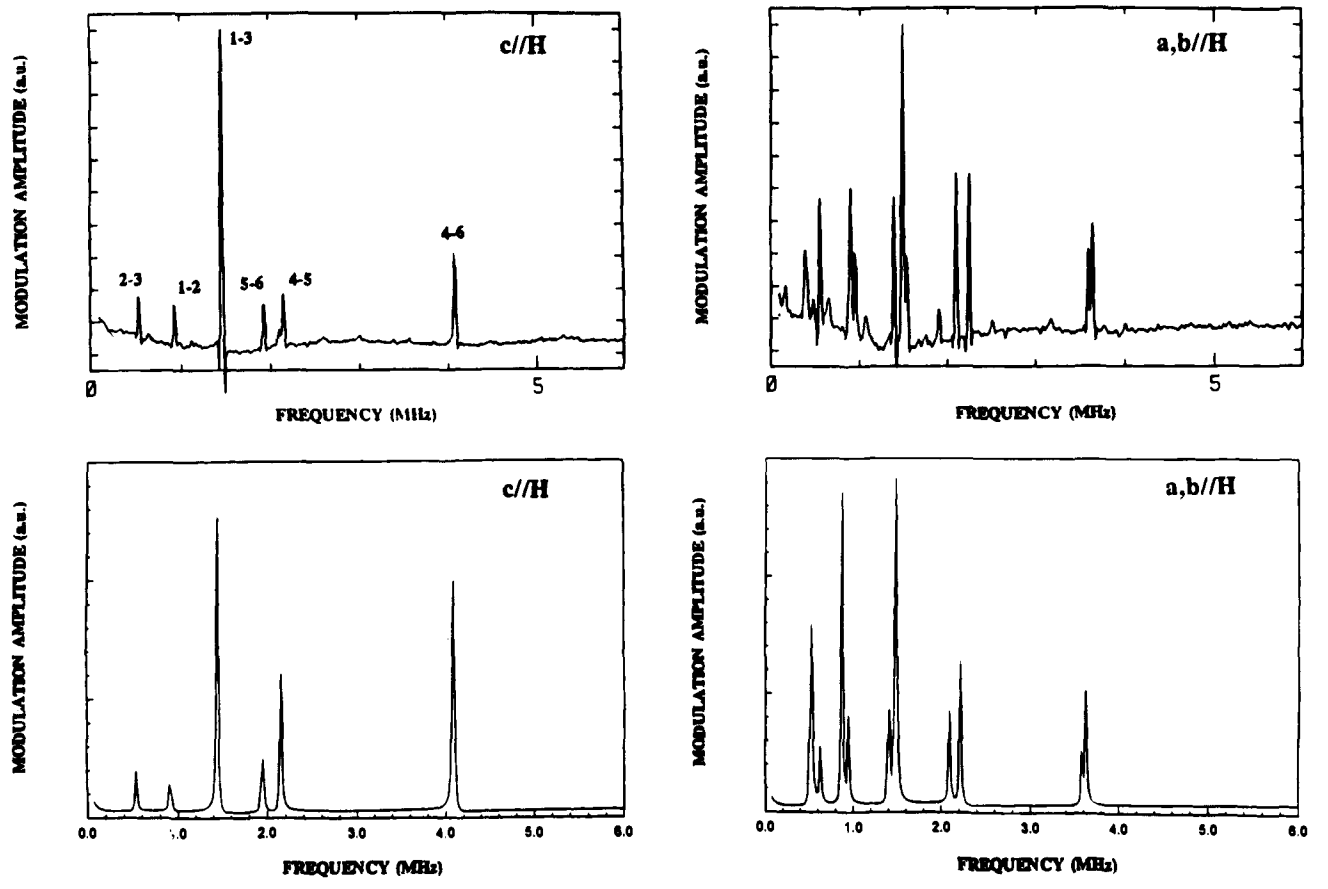

Figure 5. Upper: three-pulse FT-ESEEM patterns acquired at orientations of the magnetic field along the crystallographic axes, *c*//H and *a,b*//H. Modulation frequencies at *c*//H were 4.08, 2.15, 1.93, 1.45, 0.91, and 0.52 MHz, observed at 3131 G and 9.066 GHz with $\tau = 400$ns. Line assignments are numerated according to a scheme given in ref 5. Modulation frequencies at *a,b*//H (species A) were 3.64, 2.23, 1.47, 1.38, 0.94, and 0.55 MHz, and at *a,b*//H (species B) were 3.58, 2.09, 1.54, 1.47, 0.90, and 0.65 MHz, observed at 3042 G and 9.066 GHz with $\tau = 400$ns. Lower: Corresponding FT-ESEEM spectra simulated using the tensor parameters in Tables 1 and 2.

previously been measured by ENDOR in various copper-doped amino acid crystals.[42,45,47-50] The isotropy of the hyperfine coupling to a proton in this position has recently been proposed to follow a cosine^2 dependence on the Cu−N−C_α−H dihedral angle.[51] However, given this relationship and the magnitude of the hyperfine anisotropy that has been previously obtained by ENDOR in the above mentioned systems, the 15 MHz splitting in the present study is too large by ≈6 MHz if the C_α proton was indeed responsible for the coupling.

The larger doublet splitting in Figure 4 has a magnitude of ≈37 MHz both at *a*//H (species A) and when the external field is positioned 45° from *a,b*//H in the ab plane. There is a possibility that this splitting originates from crystal misalignment; however, identical spectra were consistently observed at X-band and at Q-band. A proton coupling to Cu(II) of this magnitude has no precedence. In addition, as shown below, no unusual complex geometry is postulated to warrant a proton to be positioned abnormally close to the Cu(II). Therefore, if this splitting does indeed reflect a proton interaction, a movement of a neighboring histidine molecule must bring a hydrogen into close proximity to the metal.

ESEEM Analysis. The three-pulse FT-ESEEM spectra with the magnetic field positioned along the *c* and *a* (or *b*) axes are depicted in Figure 5. Six major frequency lines are found at *c*//H which can be assigned to a weakly coupled nitrogen nucleus. By making ESE measurements at the field extremes of the EPR spectra, the frequency lines at *a,b*//H could be assigned to species A and B. Lines of low relative intensity arising from other coupled nuclei were frequently observed but could not be followed consistently and were therefore not analyzed. The FT-ESEEM spectra obtained along *a*//H and *b*//H were identical, as per the EPR spectra. Also, the two-fold symmetry axis along the *ab* diagonal was likewise apparent. τ-suppression experiments[34,35] were used to pair the modulation lines in the two electron spin manifolds. In addition, the lines were further assigned to give a positive a_{iso}. These six frequency lines were followed as a function of magnetic field orientation in the reference planes; the orientational dependencies are illustrated in Figure 6. Refinements of the ^{14}N coupling parameters were accomplished using these data and the results are listed in Table 2. The data rms is <0.02 MHz, and parameter uncertainties are similar to those found in previous ESEEM studies.[3,5] The solid curves in Figure 6 were theoretically generated from the listed tensors. FT-ESEEM simulations based on these tensor parameters are displayed with the observed spectra in Figure 5. All simulations were in good agreement with experimental measurements.

The ^{14}N coupling tensors obtained are comparable to those

(45) Fujimoto, M.; McDowell, C. A.; Takui, T. *J. Chem. Phys.* **1979**, *70*, 3694.
(46) Calvo, R.; Oseroff, S. B.; Abache, H. C. *J. Chem. Phys.* **1980**, *72*, 760.
(47) McDowell. C. A.; Naito, A. *J. Magn. Reson.* **1981**, *45*, 205.
(48) Bottcher, R.; Heinhold, D.; Windsch, W. *Chem. Phys. Lett.* **1977**, *49*, 148.
(49) Bottcher, R.; Heinhold, D.; Wartewig, S.; Windsch, W. *J. Mol. Struct.* **1978**, *46*, 363.
(50) Bottcher, R.; Heinhold, D.; Windsch, W. *Chem. Phys.* **1985**, *93*, 339.
(51) Colaneri, M. J.; Peisach, J. *American Crystallographic Association Annual Meeting*; 1994; Abst. PSM03.

Table 2. Remote ^{14}N Hyperfine and Quadrupole Coupling Tensors of Imidazole in Cu(II)-Doped Bis(l-histidinato)cadmium Dihydrate Determined from ESEEM Spectroscopy

principal values (MHz)	a_{iso}	direction cosines		
		a	*b*	*c*
Hyperfine Tensor				
1.97		−0.0638	0.3676	0.9278
N3(E) 1.51	1.61	0.9335	−0.3066	0.1857
1.35		0.3527	0.8780	−0.3236
Quadrupole Tensor				
0.64		0.7788	−0.5610	−0.2807
N3(E) 0.14		0.4599	0.2065	0.8636
−0.78		0.4265	0.8017	−0.4188

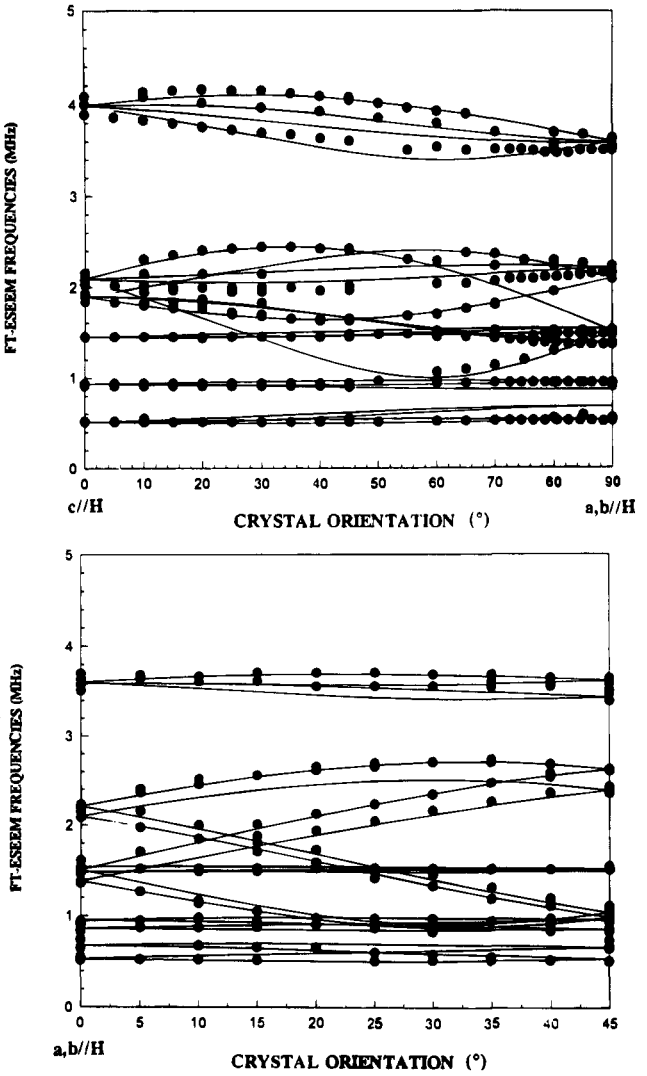

Figure 6. Plots illustrating the angular dependencies of the FT-ESEEM frequencies with the magnetic field oriented in the planes bound by the crystallographic axes. Top: With H in the plane referenced by *c*//H and *a,b*//H. Bottom: With H oriented in the *ab* plane. Solid curves depict the calculated angular dependencies of the ^{14}N FT-ESEEM frequencies using the tensors in Tables 1 and 2. For display purposes the calculated frequencies were generated assuming a smooth angular variation of the ^{14}N larmor frequency. The actual theoretical frequencies had a much better fit to the data than inferred from these plots because of their small but significant dependence on both the applied magnetic field strength and the copper nuclear spin state.

parameters previously determined for the remote nitrogen of coordinated imidazole in Cu(II)−doped L-histidine HCl H_2O.[3] This interaction therefore originates from a similarly coupled, imidazole remote ^{14}N. The present ESEEM analysis demonstrates that only one imidazole ligates to Cu(II). This is further supported by the absence of combination frequency lines[34b] in the FT-ESEEM spectra which have appreciable intensity in simulated spectra when considering two equivalent nitrogen couplings. One of the ^{14}N hyperfine interactions observed in the EPR spectra is thus due to a directly coordinated imidazole nitrogen and the other must arise from an amino nitrogen.

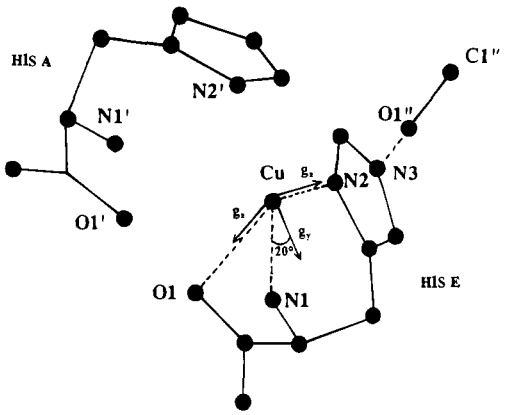

Figure 7. Proposed Cu(II) site in bis(L-histidinato)cadmium dihydrate. The two histidine molecules displayed are designated as E and A. Coordinates of the E molecule are related to the reported coordinates (A molecule) by the symmetry operation *y,x,−z*. The copper coordinates predominantly to one histidine (molecule E), equatorially through the imidazole (N2) and amino (N1) nitrogens and axially to a carboxyl oxygen. A carboxyl oxygen (O1') from the neighboring histidine (molecule A) is probably positioned trans to the imidazole nitrogen ligand by a small rotation (≈20°) about the C3(A)−C2(A) bond. Good correlations are found between the g_x, g_y, and g_z component directions and the Cu(II)−N2(E), Cu(II)−N1(E), and Cu(II)−O1(E) directions, respectively. ESEEM spectroscopy was used to obtain the hyperfine and quadrupole coupling tensors of the remote imidazole nitrogen, N3(E).

Discussion

Proposed Cu(II) Binding Site. The quadrupole tensor principal axis system in Table 2 correlates with only one of the eight possible imidazole remote ^{14}N bonding orientations in the crystal lattice. This site is designated as E in the crystal structure and is related to the reported coordinates (site A) by the symmetry operation: *y,x,−z*. Figure 7 depicts the histidine molecules that correspond to sites A (primed atoms) and E (unprimed atoms), which, incidently, form a pair that coordinate to the cadmium ion in the host structure. The minimum (−0.78 MHz), intermediate (0.14 MHz) and maximum (0.64 MHz) quadrupole tensor values each occur within 4−6° of the imidazole plane normal, the >N3(E)−H8(E) bond direction and the perpendicular to these two directions, respectively. The close correspondence of the quadrupole tensor with the remote nitrogen geometry of imidazole indicates that the imidazole moiety is not significantly disturbed from its position in the structure upon copper ligation.

The direction cosines with respect to the *a*, *b*, and *c* axes associated with the O1(A)−N2(E) and N1(A)−N1(E) vectors in the crystal structure[27] are (0.1449, 0.7733, 0.6173) and (0.6569, −0.6569, 0.3701), respectively. The plane normal defined by the cross product of the O1(A)−N2(E) and N1(A)−N1(E) directions is 5° from the g_z direction. In addition, the g_x (2.048) and g_y (2.092) directions are 4° and 8° from the N2(E)−O1(A) and N1(E)−N1(A) directions, respectively. The copper ion is thus approximately in the N2(E)−O1(A)−N1(E)−N1(A) plane. The proposed Cu(II) position, in fractional units, is 0.2305, 0.1555, −0.003. Figure 7 displays the proposed Cu(II) binding site in the crystal lattice. At this site, the copper ion

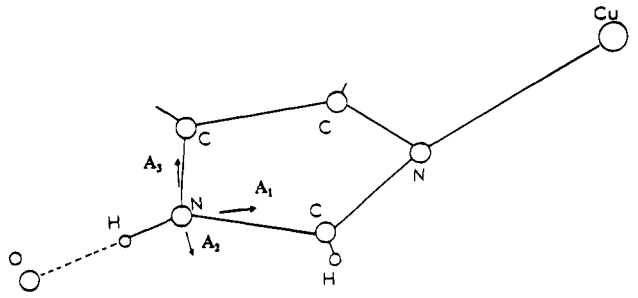

Figure 8. The orientation of the remote ^{14}N hyperfine coupling tensors with respect to the imidazole and Cu(II) geometries in the doped L-histidine HCl H_2O[3] (II) and bis(L-histidinato)cadmium dihydrate (I) crystal systems. For II, the anisotropic components of the hyperfine tensor are $A_1 = 0.37$, $A_2 = -0.09$, and $A_3 = -0.28$ MHz, with the A_3 and A_1 tensor component directions making angles of 8° with the imidazole plane normal and 13° with the imidazole Nδ−Nϵ direction, respectively. For I, the anisotropic components are $A_1 = 0.36$, $A_2 = -0.10$, and $A_3 = -0.26$ MHz, with the A_3 and A_1 component directions making angles of 4° with the imidazole plane normal and 10° from the imidazole Nδ−Nϵ direction, respectively.

has equatorial ligand interactions with the N2(E) and N1(E) at distances of 2.01 and 2.03 Å, respectively and direction cosines of 0.1615, 0.7494, 0.6421 for Cu(II)−N2(E) and 0.8753, 0.2197, −0.4309 for Cu(II)−N1(E). In addition, the N2(E)−Cu−N1(E) angle is 105°, and the normal defined by N2(E)−Cu−N1(E) is 11° from the direction of g_z. The O1(E) oxygen occupies an axial ligand position at a distance of 2.36 Å from Cu(II). The deviation of the g_z direction from the Cu(II)−O1(E) contact direction is 3°. The occupation of ligands at the two other equatorial positions is a matter of conjecture. Cu(II) contact distances of 2.6 Å for N1(A) and 2.7 Å for O1(A) in the undisturbed crystal structure are both too long to be considered ligand interactions. Since there is no precedence for a two ligand−Cu(II) complex, it seems unlikely that weak interactions at the two other remaining equatorial ligand positions can stabilize the complex. A Cu(II)−amino acid complex containing three equatorial ligands has, however, been identified by EPR[39,47] and ENDOR[47] spectroscopy. Thus, a more probable model is one where atoms from neighboring molecules move so to occupy at least one of the unassigned ligand positions. For example, a small rotation of 20° about the C2(A)−C3(A) bond moves carboxylate O1(A) from 2.7 to 2.1 Å from the proposed Cu(II) site. The rotated O1(A) remains almost exactly trans to the imidazole N2(E) (the O1(A)−Cu−N2(E) angle is 175°) while remaining in the g-tensor, xy plane.

There are six carbon bound hydrogens within 4 Å of the Cu(II) site. Two of these hydrogens (H4) are bound at imidazole Cϵ positions. EPR spectra obtained from crystals grown in D_2O with the Cϵ protons exchanged with deuterons were indistinguishable from spectra obtained from crystals grown in D_2O. The closest of the four remaining nonexchangeable protons is H3(E) at a distance of ≈3.4 Å. The H3(E) proton is notable in that it is situated close to the plane containing the unpaired electron. However, the large Cu−H distance precludes the possibility for a significant amount of spin delocalization to this proton. The next closest is the C2(E) hydrogen (H1) at ≈3.6 Å which has been alluded to above. The other two hydrogens, bound to C2 from neighboring histidines, are at longer distances of 3.8 and 3.9 Å.

The Remote ^{14}N Coupling Tensors. The anisotropic components (0.36, −0.10, −0.26) MHz of the remote ^{14}N hyperfine tensor are essentially the same as those previously determined in Cu(II)-doped L-histidine HCl H_2O (0.37, −0.09, −0.28) MHz.[3] As illustrated in Figure 8, the corresponding hyperfine tensor principal directions with respect to the imidazole geometries are within 4° of each other. Thus in the two histidine crystal systems studied, a notable similarity was found for the ^{14}N hyperfine tensor anisotropy in its predominant rhombic form (A, 0, −A), magnitude (0.37, −0.09, −0.27 MHz), and directionality with respect to the imidazole moiety. On closer examination, an additional similarity is revealed in these two systems. These are the approach of the copper ion with respect to the imidazole moiety. Specifically, the copper ligates to the imidazole moiety ≈25° from the C−N−C angle bisector and ≈65° from the plane normal.

On the other hand, the ^{14}N quadrupole coupling parameters, $e^2qQ/h = -1.57$ MHz and $\eta = 0.64$, are significantly different than those obtained previously in Cu(II)-doped L-histidine HCl H_2O,[3] $e^2qQ/h = 1.41$ MHz and $\eta = 0.66$. A Townes−Dailey analysis[52] of the quadrupole tensor, similar to that performed previously,[3] yields the following electronic valence orbital occupancies; a (occupancy in the nitrogen orbital directed along the N−H bond) = 1.284 and c (occupancy of p-π nitrogen orbital) = 1.326. These can be compared to those previously found in the Cu(II)-doped L-histidine HCl H_2O system: $a = 1.362$, $c = 1.312$.[3] The significantly lower orbital occupancy in the N-H bond may reflect the weaker hydrogen bond found in bis(L-histidinato)cadmium dihydrate structure[35] as compared to the L-histidine HCl H_2O host system.[53]

Conclusion

The correlation of the tensor components listed above, that is, to the same site in the structure provides corroborative information for the postulation of a copper binding site. The copper substitutes the Cd(II) ion but not isomorphously. EPR spectra show two ^{14}N couplings that have interactions consistent with directly coordinated nitrogens. EPR obtained tensors indicate a copper $d_{x^2-y^2}$ ground state with a dominating square-planar crystal field. ESEEM results show that one imidazole ligates to the copper ion and does not move significantly away from its position in the host structure. A good correspondence is found between the g_x and g_y principal directions and the Cu−N(imid) and Cu−N(amino) contact directions, respectively. The axial carboxylate O1 oxygen to Cu(II) vector is closely aligned with the g-tensors' maximum direction. Copper coordination is therefore predominantly to one histidine molecule, with equatorial ligands consisting of the imidazole and amino nitrogens, and the carboxylate O1 oxygen positioned axially.

Histidine has been found to act as both a bidentate and tridentate ligand in copper−histidine crystal structures.[6-14] As described above, the proposed copper binding in the present system is in accord with the tridentate mode of coordination. A major difference between the present model and all the copper−histidine crystal structures is the number of equatorial ligands. A possible reason for the absence of a fourth equatorial copper ligand in the present study is crystal packing or steric constraints on the site. The complex can therefore be construed as being of lower stability than say a four-coordinated copper complex. An observation in support of this contention is a temperature dependence of the EPR pattern. EPR spectra measured at room temperature are found to be dramatically different than those observed at 77 K. Figure 9 displays the Q-band spectrum of crushed crystal samples of Cu(II)-doped bis(L-histidinato)-cadmium dihydrate. The stick diagrams beneath the spectral components ($g_1 = 2.186$, $g_2 = 2.169$, $g_3 = 2.084$, $A_1 = -264$ MHz, $A_2 = -212$ MHz, $A_3 = 86$ MHz) represent the EPR

(52) Townes, C. H.; Dailey, B. P. *J. Chem. Phys.* **1949**, *17*, 782.
(53) Fuess, H.; Hohlwein, D.; Mason, S. A. *Acta Crystallogr.* **1977**, *B33*, 654.

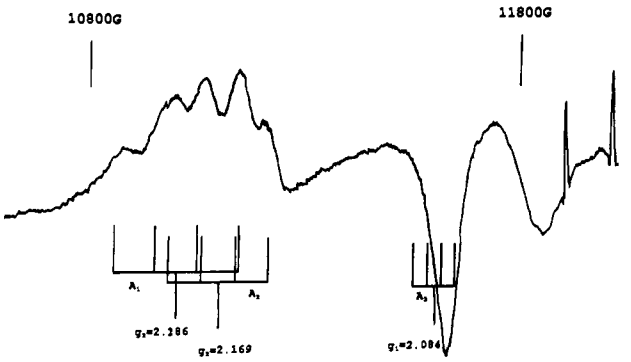

Figure 9. Q-band EPR spectra of crushed crystals ^{63}Cu(II)-doped bis-(L-histidinato)cadmium dideuterate at room temperature. The stick spectra represent g and copper hyperfine tensor components which are derived from averages of the 77 K obtained tensors. These low temperature tensors correlate with the E and A copper sites in the structure. The sharp lines at high field are due to a Mn^{2+} contaminant in the sample tubes.

parameters arrived at by averaging the 77 K measured g-tensor and ^{63}Cu hyperfine tensor. The average is taken over those tensors related by the 2-fold rotation axis positioned along the *ab* angle bisector. X-band EPR rotational measurements of single crystals at room temperature also give tensors consistent with the averaged parameters. In the cadmium structure, this 2-fold axis relates the histidine molecules that coordinate the metal. The proposed copper positions corresponding to these two histidines are within 0.9 Å of each other, and the tensor averaging is believed to occur by the metal rapidly hopping rapidly between these sites at room temperature. Interestingly, in Cu(II)-doped L-alanine, where a three coordinate complex was postulated, differences between low and room temperature EPR patterns have also been observed.[54]

The two doublet splittings observed in the EPR may arise from couplings to nonexchangeable protons in the vicinity of the Cu(II). An ENDOR investigation of this crystal would provide definitive information regarding these splittings as well as further refining the proposed copper site.

(54) Fujimoto, M.; Wylie, L. A.; Saito, S. *J. Chem. Phys.* **1973**, *58*, 1273.

Variations in the nuclear quadrupole parameters for the remote nitrogen of copper coordinated histidine imidazole observed by ESEEM in copper proteins have been attributed to differences in hydrogen-bonding interactions.[55] On the other hand, Goldfarb et al.[4] suggested that the narrow range in these parameters exhibited by type-I copper sites versus the larger range of values exhibited in type-II copper sites is due to the structural inequivalence of the imidazole nitrogens in histidine. As mentioned earlier, the two histidine crystal systems studied by ESEEM serve as models for both type-I and type-II copper sites in proteins. In Cu(II)-doped L-histidine HCl H_2O, the imidazole ligates to copper by its Nϵ nitrogen which is similar to that found in type-II sites in copper proteins, whereas in the present system, the copper coordinates to the Nδ nitrogen of imidazole, which is like that found in type-I copper proteins. Although the quadrupole tensor parameters obtained for these two crystal systems are different from each other (e^2qQ/h = 1.40 MHz, η = 0.66 for L-histidine HCl H_2O and e^2qQ/h = −1.57 MHz, η = 0.64 for bis(L-histidinato)Cd $2H_2O$), they are also significantly dissimilar to those parameters evaluated from ESEEM studies of type-I copper proteins in frozen solutions ($|e^2qQ/h|$ = 1.45−1.49 MHz, $\eta \approx$ 0.92−0.94).[4,55] Thus, the differences observed for the remote nitrogen's quadrupole parameters between type-I and type-II copper sites cannot be attributed solely to the intramolecular inequivalence of the two imidazole nitrogens of histidine.

Given the differences in the unpaired orbital and coordination in Cu(II)-doped bis(L-histidinato)cadmium dihydrate and in Cu(II)-doped L-histidine HCl H_2O, it may be concluded that both the predominant rhombic form (A, 0, −A) and the molecular principal directions of the remote nitrogen hyperfine tensor should exist for other copper−histidine complexes, such as those occurring in copper proteins.

Acknowledgment. We would like to thank Dr. Jacqueline Vitali for many helpful discussions. This work has been supported by U.S. P. H. S. Grants RR-02583 and GM-40168 to J. Peisach.

JA9501981

(55) Jiang, F.; McCracken, J.; Peisach, J. *J. Am. Chem. Soc.* **1990**, *112*, 9035.